RSC Advances

ROYAL SOCIETY OF CHEMISTRY

www.rsc.org/advances

Journal Name

RSCPublishing

ARTICLE

Microwave assisted synthesis, crystal structure and modelling of cytotoxic dehydroacetic acid enamine: a natural alkaloid from *Fusarium incarnatum* (HKI0504)

Cite this: DOI: 10.1039/xoxxoooooox

Received ooth January 2012,
Accepted ooth January 2012

DOI: 10.1039/xoxxoooooox

www.rsc.org/

Julio A. Seijas,*[a] José Crecente-Campo,[a] and Xesús Feás,[a] and M. Pilar Vázquez-Tato*[a]

A novel, fast and efficient method for the synthesis of (3*E*)-3-(1-aminoethylidene)-6-methyl-3,4-dihydro-2H-pyran-2,4-dione, a natural antiproliferative and cytotoxic product isolated from *Fusarium incarnatum* (HKI0504), was developed from dehydroacetic acid and urea under solvent-free microwave irradiation. The analysis of the co-crystal structure revealed an asymmetric unit formed by a pair of molecules. Each molecule is joined by two different hydrogen bonds to another two molecules, ordered as four-unit clusters linked by π-stacking, assembled in a brick like layered structure in a set of parallel walls. Besides, the preferred tautomer for crystal structure is the enamine form. This is corroborated by computational NBO analysis, outlining the contribution of enamine resonance and modelling the non-covalent interactions involved by means of Hirshfeld surfaces and G09 counterpoise calculations.

Introduction

Fungal endophytes are receiving growing attention due to their diverse and structurally multifarious compounds which make them interesting candidates for drug discovery. *Fusarium* is one of the most important genera of fungi, causing an array of plant diseases, producing a wide range of toxins and adversely affecting human and animal health.[1]

Recently, [(3*E*)-3-(1-aminoethylidene)-6-methyl-3,4-dihydro-2H-pyran-2,4-dione)] (**1**) has been identified as a natural product which was isolated from the culture broth of *Fusarium incarnatum* (HKI0504), an endophytic fungus of the mangrove plant *Aegiceras corniculatum*.[2] It showed antiproliferative activity against human umbilical vein endothelial cells (HUVEC), K562 human chronic myeloid leukemia cells (DSM ACC 10) and cytotoxicity against HeLa human cervix carcinoma (DSM ACC 57) cell lines. This endophyte also has been identified as a novel producer of laccase with potential in bioremediation of bisphenol A.[3]

Compound **1** is an enamine derivative of dehydroacetic acid, (3-acetyl-4-hydroxy-6-methyl-2H-pyran-2-one, **2**). Dehydroacetic acid acts as complexing ligand and possesses interesting biological properties such as fungicide and antibacterial activities.[4] Its sodium salt is recognized by Food and Agriculture Organization (FAO) and the World Health Organization (WHO) as a safe food preservative, since it has a relatively broad spectrum of antibacterial activity against food-borne pathogens and spoilage organisms. Its enamine derivatives have also been object of wide studies, because of their different biological activities and ability to act as ligands in transition metal complexes.[5]

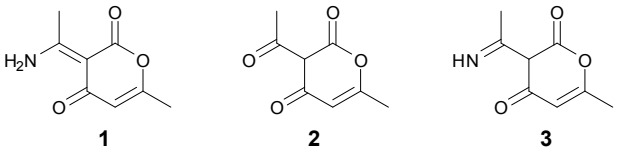

Figure 1 Dehydroacetic acid enamine (**1**), dehydroacetic acid (**2**), dehydroacetic acid imine (**3**)

Results and discussion

The product of the reaction of dehydroacetic acid and ammonia is known since 1876,[6] and several preparations were reported afterwards,[7] although the first completely reported synthesis was that of Wang et al.[8] where **1** was prepared by reaction of dehydroacetic acid with aq. NH_3 for 3 days at room temperature. Our experience in the enhancement of organic reactions by microwaves, led us to consider the possibility to improve the synthetic method using urea instead of NH_3, since it had proved to be a suitable source of ammonia under microwave irradiation for the synthesis of imides and enamines.[9] Thus, a stoichiometric mixture of dehydroacetic acid and urea was irradiated, without adding any solvent, at 150 ºC for 15 minutes in a monomode microwave oven (200 W power), yielding 85% of **1** after purification by column chromatography. As expected, this preparative method is a competitive alternative to non-assisted microwave synthesis.

The crystallization of the synthetized compound **1** from methanol, rendered a crystal whose structure was resolved resulting in a non-merohedral twin with the twin components related by a 180.0 degree rotation about the [1 0 0] axis. TWINABS was used to apply post-collection corrections. Both twin components were employed in corrections and overlaps in addition to the two components were included in the reflection file. An extra parameter was included on the refinement to properly calculate the twin ratio 0.58(2)/0.42(2). Asymmetric unit (AU, Fig.2) has two components with slightly different geometries (Table 1).

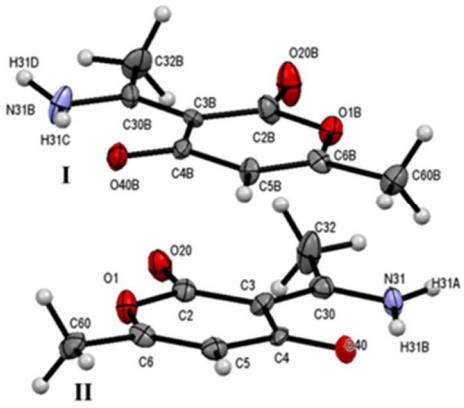

Figure 2 Molecules **I** and **II** in Asymmetric Unit of **1**

Table 1 Selected bond distances of **1**

Molecule II	Å	Molecule I	Å [% II to I]
O_1—C_6	1.377(6)	O_{1B}—C_{6B}	1.360 (6) [101.3]
C_3—C_{30}	1.420 (7)	C_{3B}—C_{30B}	1.430 (7)[101.0]
C_3—C_4	1.448(6)	C_{3B}—C_{4B}	1.426 (7)[101.5]
C_{30}—N_{31}	1.308 (7)	C_{30B}—N_{31B}	1.312 (6)[100.3]
C_{30}—C_{32}	1.488 (7)	C_{30B}—C_{32B}	1.490 (7)[100.1]

The analysis of the co-crystal[10] confirms that the structure of both components in solid state correspond to enamine (**1**) rather than to imine (**3**) which agrees with previous studies carried out on this kind of compounds.[11] The two molecules in AU are bonded through π-stacking interaction. The value of this interaction (14.18 Kcal/mol) was calculated with Gaussian09 (MP2/6-311++G(2d,2p) method) with counterpoise correction,[12] using the coordinates determined from the co-crystal.

Each molecule of the AU has also π-stacking with a molecule (**II**') in the upper face and with another (**I**') in the bottom (Fig. 3). The calculated energies for these interactions were 15.01 and 14.93 Kcal/mol respectively.

In order to study the slight variation between the two components of the AU, the energy of these molecules was calculated separately (B3LYP/6-311++G(2d,2p)). For one component of the pair (Fig. 3, molecule **I**) the Hartree-Fock energy was -590.8085 a.u. with a dipole moment of 1.87 D. The other component of the asymmetric unit (Fig. 3, molecule **II**) rendered HF= -590.8079 a.u. and a dipole moment of 2.00 D. The difference of energy between both is negligible (0.348 Kcal/mol).

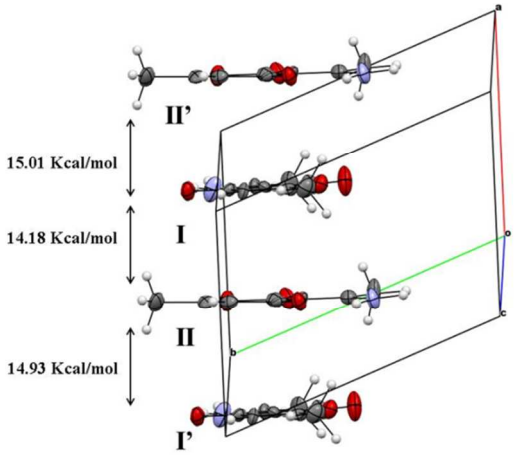

Figure 3 Molecules **I** and **II** are inside AU. Molecules **I'** (-1+x,y,z) and **II'** (1+x, y, z) belong to different AU's.

Analysis of the co-crystal shows that each molecule is part of a four-molecule cluster joined by hydrogen bonds. Since enamine **1** contains one donor and two different acceptors of hydrogen (Fig. 4a), three types of hydrogen bonding are observed (Fig. 4b): (i) intramolecular bonds $N_{31B}\cdots O_{40B}$ and $N_{31}\cdots O_{40}$ (corresponding to molecules **II** and **I** respectively), (ii) intermolecular between the amino and the ketone group $N_{31}\cdots O_{40B}$ and (iii) intermolecular between the amino group and the lactone $N_{31B}\cdots O_{20}$. The values for intermolecular hydrogen bonds (Table 2), fall inside the category of moderate mostly electrostatic of hydrogen bonds with donor-acceptor as defined by Jeffrey.[13]

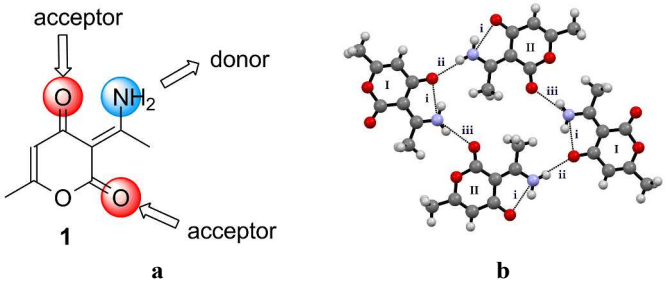

Figure 4 (a) Acceptor and donor sites in compound **1**, (b) (i) Intra- and (ii-iii) inter- molecular hydrogen bonds present in four molecules-cluster.

Table 2 Hydrogen bonds of **1** (Å, º).

Hydrogen bond	D−H	H···A	D···A	D−H···A
$N_{31}–H_{31B}···O_{40}$	0.89 (2)	1.81 (4)	2.58 (6)	143 (5)
$N_{31}–H_{31A}···O_{40B}$ [a]	0.90 (5)	2.06 (5)	2.94 (6)	168 (6)
$N_{31B}–H_{31C}···O_{40B}$	0.90 (2)	1.78 (3)	2.59 (6)	148 (5)
$N_{31B}–H_{31D}···O_{20}$ [b]	0.90 (2)	2.08 (4)	2.85 (6)	143 (5)

Symmetry codes: [a] x-1, y-1,z; [b] –x+1, -y+2, -z

The calculated total interaction energy of this cluster (MP2/6-311++G(2d,2p)) was 35.49 Kcal/mol (i.e. 8.87 Kcal/mol per each pair of molecules). The different types of intermolecular hydrogen bond were studied separately. A couple of molecules joined by $CO_{lactone}$-hydrogen present an interaction of 7.997 Kcal/mol, meanwhile for CO_{ketone}-hydrogen is 6.568 Kcal/mol. The sum of these energies indicates an additional stabilization of 6.640 Kcal/mol when the four molecules cluster is considered.

Note that these four molecules have their rings in the same plane and these small clusters are arranged as bricks in a wall, besides all the clusters in a tier have their atoms in the same plane. Thus, two bricks in a tier are bounded by π-staking (mortar) to one brick (four-molecule cluster) in the upper tier (Fig. 5a), building the wall (Fig. 5b). A plane is separated 3.321 Å from the next parallel plane in the same wall. Planes in vicinal walls are deviated 1.129 Å (Fig. 5c), and the tiers share planes each three walls, showed with a dotted line in figure 4d, where is also shown the orientation of the clusters walls inside BFDH predicted morphology of the co-crystal.

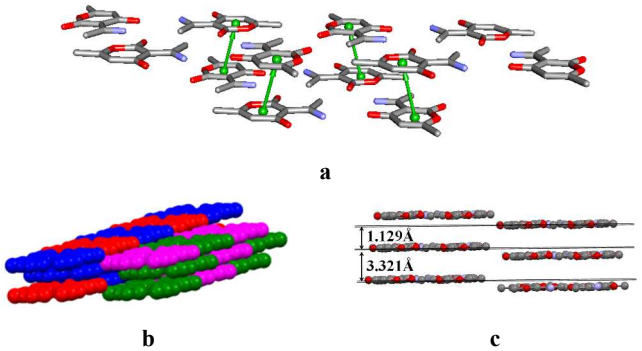

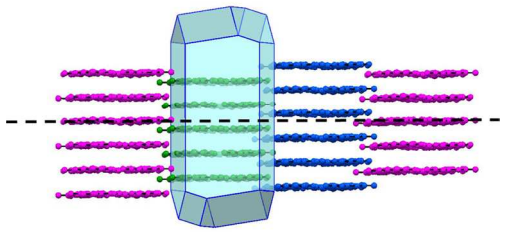

Figure 5 (a) π-stacking interaction between several four-molecules clusters. (b) Wall built with clusters (bricks), each color represents a four-molecules cluster. (c) Distances between planes defined by the clusters (d) Tiers share planes (dotted line), each three walls, and predicted BFDH morphology of the co-crystal.

The Hirshfeld surface is defined in a crystal as that region around a molecule where the molecule contribution to the crystal electron density exceeds that from all other molecules in the crystal. It allows analyzing how molecules interact with their direct environment.[14]

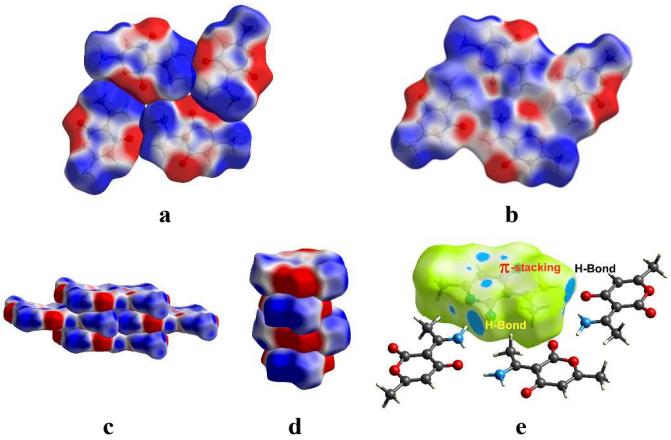

Figure 6 Hirshfeld surfaces mapped with electrostatic potentials (a) individual surfaces in the four molecules cluster, (b) integrated surface for the cluster, (c) surfaces of the clusters in a wall like bricks, (d) individual molecular surfaces showing π-stacking (see Fig. 3), (e) d_{norm} surface displaying close contacts of hydrogen bonding and π-stacking.

When the cluster of four molecules is represented by their corresponding Hirshfeld surfaces[13] with electrostatic potential mapped on it,[15] the interactions among them are clearly shown as complimentary, those individual surfaces can be integrated in a four molecules common surface (Fig. 6a-b), being its arrangement in a wall as bricks (Fig. 6c). Figure 6d shows the disposition of the electrostactic potential mapped on Hirshfeld surfaces of the π-stacked molecules represented in figure 2. The d_{norm} surfaces (Fig. 6e), reveal the close contacts of hydrogen bond donors and acceptors represented in figure 4b. The large circular depressions (cyan) are the indicators of hydrogen bonding contacts. The dominant O···H-N interactions are evident in the Hirshfeld surface and confirm the nature of the binding forces inside the cluster, π-stacking can also be observed with the upper row of molecules.

Table 3 Principal donor-acceptor interactions between NBO

Entry	Donor bond	Isovalue 95%	Acceptor bond	Isovalue 95%	(E2) Kcal/mol
1	42. n_{N31}	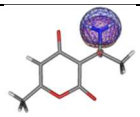	484. π_{C3-C30}*	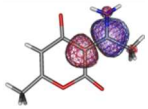	72.03
2	8. π_{C3-C30}	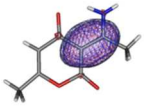	481. π_{C2-O20}*	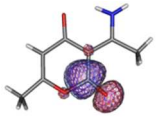	39.33
3	8. π_{C3-C30}	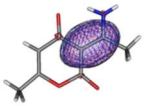	487. π_{C4-O40}*	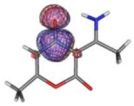	37.91
4	39. n_{O1}	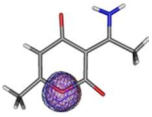	481. π_{C2-O20}*	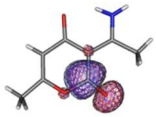	32.81
5	39. n_{O1}	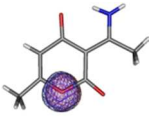	490. π_{C5-C6}*	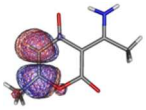	31.64
6	14. π_{C5-C6}	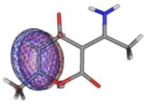	487. π_{C4-O40}*	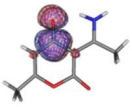	24.90
7	44. n_{O40}	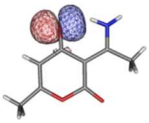	494. $\sigma_{N31-H31B}$*	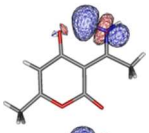	10.68
8	43. n_{O40}	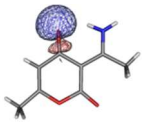	494. $\sigma_{N31-H31B}$*		2.12

Natural bond orbital (NBO) analysis of dehydroacetic acid derivatives has proved to be a useful way for understanding the structure of β-enaminones.[11] Now, the knowledge of the crystal structure of **1** will allow a better comparison between experimental and calculated data. Thus, the study of the properties in gas phase (b3lyp/6-311++G(2d,2p)) of the more stable component of the AU (molecule **I**, Fig. 1) was carried out. In this analysis (Table 3), stabilization energy E(2) related to the delocalization trend of electrons from donor to acceptor orbitals, is calculated via perturbation theory. Thus, NBO calculation using Gaussian09 indicated that the highest interaction correspond to orbitals $n_{N31} \rightarrow \pi_{C3-C30*}$ characteristic of the enamine structure, according to data from X-ray. The next higher energy interactions were $\pi_{C3-C30} \rightarrow \pi_{C2-O20*}$ and $\pi_{C3-C30} \rightarrow \pi_{C4-O40*}$ resulting from conjugation of the enamine double bond with both carbonyl groups. The lone pair of the oxygen in the ring is delocalized with the lactone carbonyl and the endocyclic alkene: $n_{O1} \rightarrow \pi_{C2-O20*}$ and $n_{O1} \rightarrow \pi_{C5-C6*}$. Furthermore, the delocalization $\pi_{C5-C6} \rightarrow \pi_{C4-O40*}$ supports the β-enaminone structure.

The principal donor-acceptor interactions between NBO orbitals are summarized in Table 3, showing the surfaces whose isovalue represents 95% of the orbital, so the effectiveness of the overlapping can be visualized.

The electronic conjugation in molecules was studied by Wiberg bond indexes,[16] the results showed that C_3-C_{30} and C_{30}-N_{31} bonds have higher values than single bonds as C_{30}-C_{32} (Fig. 7). So, this structure could be represented as a three centre delocalized bond in C_3-C_{30}-N_{31}.

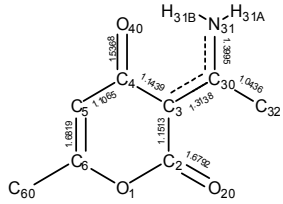

I

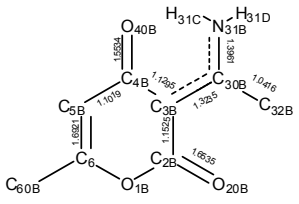

II

Figure 7 Wiberg bond indexes for molecules **I** and **II** in AU, dashed lines indicate three centre delocalized bonds.

As it is known, theoretical calculations of magnetic properties can be performed through different methods. The most widely used for this type of calculation is the GIAO method,[17] where a source of potential vector of the external magnetic field for each atom is settled independently. Therefore, the coordinates of the structure derived from X-ray data were used to calculate NMR proton shifts (b3lyp/6-311++G(2d,2p)) by this method in the gas phase. The absolute shielding returned by the program was transformed in chemical shifts subtracting the absolute shielding of TMS from the absolute shielding of the molecule. However, the theoretical shifts obtained did not match with the experimental values. GIAO method may include the effect of solvent, and the polarizable continuum model (PCM) is generally used.[18] Therefore, the presence of solvent was considered by placing the solute (coordinates from X-ray structure) in a cavity within the solvent reaction field (PCM). The results from this model implemented in Gaussian 09 also showed no accuracy; this could be due to the intermolecular hydrogen bonding present in the crystal. A refined molecular structure was calculated by minimizing the crystal structure with PCM model in chloroform; in this case the shifts (GIAO-PCM) were similar to experimental (Table 4).

Table 4 NMR proton shifts (δ, ppm)

Crystal coord. GIAO-($CDCl_3$) ^{1}HNMR		Crystal coord. GIAO-($CDCl_3$) ^{1}HNMR		Crystal coord. minimized ($CDCl_3$) GIAO-($CDCl_3$)	
I	δ	**II**	δ	δ	$\delta_{exp.}$
H_{31B}	9.51	H_{31C}	7.99	12.95	12.56
H_{31A}	3.79	H_{31D}	3.46	6.22	6.96
H_5	3.35	H_{5B}	3.46	5.97	5.70
H_{32A}	-1.71	H_{32D}	-1.75	1.71	2.65
H_{32B}	-0.39	H_{32E}	-.57	3.04	2.65
H_{32C}	-0.75	H_{32F}	-0.64	3.04	2.65
H_{60A}	-1.65	H_{60D}	-1.75	1.94	2.13
H_{60B}	-1.47	H_{60E}	-1.39	2.26	2.13
H_{60C}	-1.47	H_{60F}	-1.48	2.26	2.13

The minimized structure presented a change in the relative positions of H_{31A}, H_{31B}, H_{31C} and H_{31D} (involved in hydrogen bonding). The position of nitrogen was also modified affecting to the length of the hydrogen bonds present (Table 5).

Table 5 Interatomic distances (Å).

Hydrogen bond	Crystal X-ray **I**	Hydrogen bond	Crystal X-ray **II**	Minimized PCM/$CHCl_3$
O_{40B}---H_{31C}	1.78(3)	O_{40}---H_{31B}	1.81(4)	1.75
O_{40B}---N_{31B}	2.59(5)	O_{40}---N_{31}	2.58(5)	2.58
O_{40B}---H_{31D}	3.42(3)	O_{40}---H_{31A}	3.38(5)	3.49

The interaction between O_{40} and H_{31B} and O_{40B} and H_{31C} can be considered as an example of resonance-assisted hydrogen bond which is a model of synergistic interplay between π-delocalization and hydrogen-bond strengthening (RAHB).[19] The interatomic distances (Table 5) from crystal structure and minimized are inside the values found by Gilli for substituted β-enaminones.[20] This heteronuclear RAHB is of great chemical and biochemical relevance because chains of H-bonded amide groups determine the secondary structure of proteins. NBO analysis reflects the stabilization gained by donation from two lone pairs of O_{40} to the acceptor $\sigma_{N10\text{-}H20^*}$ being 10.68 and 2.12 Kcal/mol (Table 3, entries 7 and 8). Meanwhile, in the minimized structure the distance between N_{10} and O_{40} is shorter, leading to stabilization of 14.92 and 3.42 Kcal/mol, respectively; higher than the observed for crystal, which agrees to a stronger hydrogen bond in the structure in solution.

Experimental

General Experimental Procedures. NMR spectra were recorded on a Varian Mercury 300 7.04 T (300.13 MHz for ^{1}H and 75.48 for ^{13}C. Mass spectra were performed on a HP-Series 1100-MSD. IR spectra were performed on a ABM BOMEN MB102 on KBr pellets. For column chromatography was used 230-400 mesh silica gel. For microwave reaction a single-mode oven model CEM Discover was used.

(3E)-3-(1-aminoethylidene)-6-methyl-3,4-dihydro-2H-pyran-2,4-dione (**1**). In a 10 mL tube, dehydroacetic acid (338 mg, 2.01 mmol) and urea (126 mg, 2.1 mmol) were well mixed. The mixture was irradiated in a monomode microwave oven with stirring at 150 °C for 15 min (200 W). The reaction crude was purified by column chromatography (eluent CH_2Cl_2:MeOH, 95:5), obtaining (3*E*)-3-(1-aminoethylidene)-6-methyl-3,4-dihydro-2H-pyran-2,4-dione (283 mg, 85%), as a light yellow solid. m. p. 210-212 °C (methanol) (Lit. 210-213 °C).[21] ^{1}H-NMR (300 MHz, $CDCl_3$), δ: 12.56 (br s, 1H, NH_2), 6.96 (br s, 1H, NH_2), 5.70 (s, 1H, CH_3C=CH), 2.65 (s, 3H, CH_3C=CH), 2.13 (s, 3H, CH_3CN). ^{13}C-NMR (75 MHz, DMSO), δ: 184.0 (COCH), 177.3 (CN), 163.7 (CH_3C=CH), 162.8 (COO), 108.0 (CH_3C=CH), 96.0 (CCOO). 24.7 (CH_3C=CH), 19.8 (CH_3CN). MS m/z (%):167 (M^+, 100). 152 (20), 126 (5), 124 (10), 97 (8), 83 (74), 68 (32), 55 (23). IR υ_{max} (KBr, film): 3281 (NH_2), 1715 (COO), 1684 (CO), 1668, 1585, 1571, 1468, 1355, 1068, 1037.

X-ray Crystallographic Analysis. For compound **1**, single-crystal X-ray diffraction data were collected on an APPEX2 (BRUKER AXS, 2005); with Mo Kα radiation (λ = 0.7107 Å).The structure was solved by direct methods (SHELXS-86) and refined using SHELXL2012. X-ray data for 1 has been deposited with the Cambridge Crystallographic Data Centre: CCDC reference number CCDC 945618 This data can be obtained, free of charge, from the Cambridge Crystallographic Data Centre via http://www.ccdc.cam.ac.uk/data_request/cif. Crystal data for **1**: $C_{16}H_{18}N_2O_6$, M = 334.32, a = 6.650(3) Å, b = 8.898(4) Å, c = 13.970(6) Å, α = 92.24(2)°, β = 98.98(2)°, γ = 111.168(19)°, V = 757.3(6) Å^3, T = 100(2) K, space group $P\bar{1}$, Z = 2, μ(MoKα) = 0.113 mm^{-1}, 3506 reflections measured, 3506 independent reflections (R_{int} = 0.111). The final R_1 values were 0.0706 ($I > 2\sigma(I)$). The final $wR(F^2)$ values were 0.1431 ($I > 2\sigma(I)$). The final R_1 values were 0.1713 (all data). The final $wR(F^2)$ values were 0.1889 (all data). The goodness of fit on F^2 was 0.997. In the crystal structure coordinates for hydrogens H_{31A}, H_{31B}, H_{31C} and H_{31D} were positioned by electronic density and refined with a restraint to the length distance of 0.87Å except H_{31A} which is completely free. For more details on geometry and refinement see supplementary material.

Conclusions

This article presents an efficient solvent free microwave assisted synthesis for cytotoxic pyrandione alkaloid (3*E*)-3-(1-aminoethylidene)-6-methyl-3,4-dihydro-2H-pyran-2,4-dione, improving previously described synthesis. The study of the X-ray structure of this recently isolated natural product, shows a co-crystal with a basic four molecules cluster joined by two different types of intermolecular hydrogen bonds. These flat clusters are linked by π-stacking, adopting a brick like layered structure constituting a set of parallel walls. Besides, the preferred tautomer structure is the enamine form. This is corroborated by NBO analysis outlining the contribution of enamine resonance. The study of the Hirshfeld surfaces showed the influence of molecular electrostatic potential in the spatial disposition of the molecules. These results might be valuable for further structure–activity studies of substituted pyrandione, molecular design and synthesis of more potent and selective antiproliferative compounds.

Acknowledgements

XUNTA DE GALICIA for financial support: Grant INCITE09 262346PR. X.F. would also like to thank the Xunta de Galicia (Isidro Parga Pondal Program for young researchers, Grant No. IPP-020). Centro de Supercomputación de Galicia (CESGA) for providing computing facilities (Gaussian 09).[22]

Notes and references

[a] Departamento de Química Orgánica, Facultad de Ciencias. Universidad de Santiago de Compostela, Aptdo. 27080, Lugo, Spain

† Electronic Supplementary Information (ESI) available: [cif file for compound **1**, crystallographic tables, 1H and 13C NMR spectra for compound **1**]. See DOI: 10.1039/b000000x/

1 B. A. Summerell, J. F. Leslie, *Fungal Divers.* 2011, **50**, 135; M. Nucci, E. Anaissie, *Clin. Microbiol. Rev.* 2007, **20**, 695; R. Galimberti, A. C. Torre, M. C. Baztán, F. Rodriguez-Chiappetta, *Clin Dermatol.* 2012, **30**, 633; K. Kazan, D. M. Gardiner, J. M. Manners, *Mol. Plant. Pathol.* 2012, **13**, 399; L. V. Khoa, K. Hatai, T. Aoki, *J. Fish Dis.* 2004, **27**, 507; S. Naiker, B. Odhav, *Mycoses* 2004, **47**, 50.

2 L. Ding, H-M. Dahse, C. Hertweck, *J. Nat. Prod.* 2012, **75**, 617.

3 U. Chhaya, A. Gupte, *J. Hazard. Mater.* 2013, **254-255**, 149.

4 Y. Huang, M. Wilson, B. Chapman, A. D. Hocking, *Food Microbiol.* 2010, **27**, 33; H. Zhang, H. Wei, Y. Cui, G. Zhao, F. Feng, *J. Food Sci.* 2009, **74**, M418.

5 L. Duraković, A. Skelin, S. Sikora, F. Delaš, M. Mrkonjić-Fuka, K. Huić-Babić, M. Blažinkov, *Afr. J. Biotechnol.* 2011, **10**, 10798; S. Kiryu, *Acta Cryst.* 1967, **23**, 392; M. Laćan, I. Susnik-Rybarski, E. Mesić, H. Džanic, *Liebigs Ann. Chem.* 1980, 681; E. Budzisz, M. Malecka, I-P. Lorenz, P. Mayer, R. A. Kwiecien, P. Paneth, U. Krajewska, M. Rozalski, *Inorg. Chem.* 2006, **45**, 9688; S. Shahid, T. Mughal, H. U. Shah, *Asian J. Chem.* 2013, **25**, 633; A. S. Munde, V. A. Shelke, S. M. Jadhav, A. S. Kirdant, S. R. Vaidya, S. G. Shankarwar, T. K. Chondhekar, *Adv. Appl. Sci. Res.* 2012, **3**, 175; V. A. Shelke, S. M. Jadhav, S. G. Shankarwar, C. S. Munde, T. K. Chondhekar, *J. Korean Chem. Soc.* 2011, **55**, 436; L. C. Dias, A. J. Demuner, V. M. M. Valente, L. C. A. Barbosa, F. T. Martins, A. C. Doriguetto, J. Ellena, *J. Agric. Food Chem.* 2009, **57**, 1399.

6 A. Oppenheim *Berichte der deutschen chemischen Gesellschaft* 1876, **9**, 1099.

7 F.Feist *Berichte der deutschen chemischen Gesellschaft* 1890, **26**, 315. F. Feist *Justus Liebig's Ann. Chem.* 1890, **257**, 253. J. N. Collie, S. Myers *J. Chem. Soc. Trans.* 1893, **63**, 122. S. Iguchi, K. Hisatune, *Yakugaku Zasshi,* 1957, **77**, 98. S. Kiryu *Acta Cryst.* 1967, **23**, 392. S. Iguchi, S. Goto, Y. Kodama *J. Pharm. Soc. Jpn* 1959. **79**, 1100

8 C. S. Wang, J. P. Easterly, N. E. Skelly, *Tetrahedron* 1971, **27**, 2581.

9 J. A. Seijas, M. P. Vázquez-Tato, C. González-Bande, M. M. Martínez, B. López-Pacios, *Synthesis* 2001, 999; P. Ruault, J.-F. Pilard, B. Touaux, F. Texier-Boullet, J. Hamelin, *Synlett* 1994, 935.

10 N. Upadhyay, T. P. Shukla, .A Mathur, Manmohan, S. K. Jha, *Int. J. Pharm. Sci. Rev. Res.* 2011, **8**,144.

11 A. Amar, H. Meghezzi, A. Boucekkine, R. Kaoua B. Kolli, *C. R. Chim.* 2010, **13**, 553; S. A. Hameed, S. K. Alrouby, R. Hilal, *J. Mol. Model.* 2013, **19**, 559; P. E. Hansen, S. Bolvig, T. Kappe, *J. Chem. Soc., Perkin Trans. 2* 1995, 1901.

12 N. Kobko, J. J. Dannenberg, *J. Phys. Chem*. 2001, **105**, 1944.

13 G. A. Jeffrey, *An introduction to hydrogen bonding.* Oxford University Press: New York, 1997.

14 J. J. McKinnon, M. A. Spackman, A. S. Mitchell, *Acta Crystallogr., Sect. B: Struct. Sci.* 2004, **B60**, 627.

15 Hirshfeld surfaces were calculated using CrystalExplorer (Version 3.1, S. K. Wolff, D. J. Grimwood, J. J. McKinnon, M. J. Turner, D. Jayatilaka, M. A. Spackman, University of Western Australia, 2012) electrostatic potential was calculated using Tonto, D. Jayatilaka and D. J. Grimwood, Computational Science-ICCS 2003, 4, 142-151 in DFT calculation with a 6-311G(d,p) basis, Becke88 exchange potential and LYP correlation potential.

16 K. B. Wiberg, *Tetrahedron* 1968, **24**, 1083.

17 R. Ditchfield, *J. Chem. Phys.* 1972, **56**, 5688.

18 S. Miertus, E. Scrocco, J. Tomasi, *Chem. Phys.* 1981, **55**, 117.

19 G. Gilli, F. Bellucci, V. Ferretti, V. Bertolasi, *J. Am. Chem. Soc.* 1989, **111**, 1023; V. Bertolasi, P. Gilli, V. Ferretti, G. Gilli, *J. Am. Chem. Soc.* 1991, **113**, 4917; V. Bertolasi, L. Pretto, G. Gilli, P. Gilli, *Acta Crystallogr., Sect. B: Struct. Sci.* 2006, **B62**, 850; P. Gilli, L. Pretto, V. Bertolasi, G. Gilli, *Acc. Chem. Res.* 2009, **42**, 33. V. Bertolasi, P. Gilli, G. Gilli, *Cryst. Growth Des.* 2012, **12**, 4758. G. Gilli, V. Bertolasi, P. Gilli, *Cryst. Growth Des.* 2013, **13**, 3308.

20 P. Gilli, V. Bertolasi, V. Ferretti, G. Gilli, *J. Am. Chem. Soc.* 2000, **122**, 10405.

21 J. D. Edwards, J. E. Page, M. Pianka, *J. Chem. Soc.* 1964, 5200.

22 M. J. Frisch, G. W. Trucks, H. B. Schlegel, G. E. Scuseria, M. A. Robb, J. R. Cheeseman, G. Scalmani, V. Barone, B. Mennucci, G. A. Petersson, H. Nakatsuji, M. Caricato, X. Li, H. P. Hratchian, A. F. Izmaylov, J. Bloino, G. Zheng, J. L. Sonnenberg, M. Hada, M. Ehara, K. Toyota, R. Fukuda, J. Hasegawa, M. Ishida, T. Nakajima, Y. Honda, O. Kitao, H. Nakai, T. Vreven, J. A. Montgomery, Jr., J. E. Peralta, F. Ogliaro, M. Bearpark, J. J. Heyd, E. Brothers, K. N. Kudin, V. N. Staroverov, R. Kobayashi, J. Normand, K. Raghavachari, A. Rendell, J. C. Burant, S. S. Iyengar,. J. Tomasi, M. Cossi, N. Rega, J. M. Millam, M. Klene, J. E. Knox, J. B. Cross, V. Bakken, C. Adamo, J. Jaramillo, R. Gomperts, R. E. Stratmann, O. Yazyev, A. J. Austin, R. Cammi, C. Pomelli, J. W. Ochterski, R. L. Martin, K. Morokuma, V. G. Zakrzewski, G. A. Voth, P. Salvador, J. J. Dannenberg, S. Dapprich, A. D Daniels,. Ö. Farkas, J. B. Foresman, J. V. Ortiz, J. Cioslowski, D. J. Fox, GAUSSIAN 09 (Revision A.02), Gaussian, Inc., Wallingford CT, 2010.

